

Supporting Information for

Disulfide Reductive Elimination From an Iron(III) Complex

Janice L. Wong,^a Raúl Hernández Sánchez,^b Jennifer Glancy Logan,^a Joseph W. Ziller,^a Ryan A. Zarkesh,^a Alan F. Heyduk^{*, a}

^a *Department of Chemistry
University of California, Irvine, California, 92697, USA*

^b *Department of Chemistry and Chemical Biology
Harvard University, Cambridge, Massachusetts, 02138*

	Page
Experimental Section	S2
Figures S1-S2. EPR and Mössbauer spectra of $[\text{ONO}^q]\text{FeCl}_2$ (1).	S3
Figures S3. EPR spectrum of $[\text{ONO}^q]\text{Fe}[\text{N}(\text{SiMe}_3)_2]_2$ (2).	S4
Figure S4. EPR spectrum of $[\text{ONO}^q]\text{Fe}(\textit{ortho}\text{-C}_6\text{O}_2\text{Cl}_4)(\text{py})$ (3).	S5
Figures S5-S6. EPR and Mössbauer spectra of $[\text{ONO}^{\text{cat}}]\text{Fe}(\text{py})_3$ (5).	S6
Figure S7-S8. Quantification of di- <i>tert</i> -butyl disulfide and azobenzene.	S7
Crystallographic Methods	S9
Figure S9-S10. ORTEP diagrams of $\{[\text{ONO}^q]\text{Fe}(\textit{ortho}\text{-C}_4\text{O}_2\text{Cl}_4)\}_2$ (4) and $\{[\text{ONO}^{\text{cat}}]\text{Fe}(\text{py})\}_2$ (6).	S10
Table S1. X-Ray Diffraction Data Collection and Refinement Parameters for $[\text{ONO}^q]\text{FeCl}_2$ (1), $[\text{ONO}^q]\text{Fe}[\text{N}(\text{SiMe}_3)_2]_2$ (2), $[\text{ONO}^q]\text{Fe}(\textit{ortho}\text{-C}_6\text{O}_2\text{Cl}_4)(\text{py})$ (3), $\{[\text{ONO}^q]\text{Fe}(\textit{ortho}\text{-C}_4\text{O}_2\text{Cl}_4)\}_2$ (4), $[\text{ONO}^{\text{cat}}]\text{Fe}(\text{py})_3$ (5), and $\{[\text{ONO}^{\text{cat}}]\text{Fe}(\text{py})\}_2$ (6).	S11
References	S12

Experimental

General Procedures. All compounds and reactions reported below were carried out under air- and moisture-free conditions using standard glovebox or Schlenk techniques. Solvents were sparged with nitrogen and then deoxygenated and dried by passage through Q5 and activated alumina columns, respectively. To test for effective oxygen and water removal, solvents were treated with a few drops of a purple solution of sodium benzophenone ketyl in THF. The C₆D₆ NMR solvent was dried over sodium-potassium amalgam benzophenone ketyl for two days, followed by trap-to-trap vacuum distillation and several freeze-pump-thaw cycles. The compounds potassium graphite (KC₈), ¹ [ONO^{cat}]₃H₃, ² K[ONO^q], ³ 1,2-bis(4-methylphenyl)diazene,⁴ and FeCl(THF)[N(SiMe₃)₂]₂⁵ were synthesized according to published procedures. The FeCl₃ was purchased from Strem and used without further purification. Diphenylhydrazine and azobenzene were purchased from Alfa Aesar and sublimed before use. The pyridine (Macron), *tert*-butylthiol (Alfa Aesar), diisopropyl disulfide (Acros), and di-*tert*-butyl disulfide (Acros) were dried over activated 4 Å molecular sieves (Fisher Scientific) overnight and then distilled under reduced pressure into a Straus flask and degassed through several freeze-pump-thaw cycles. Potassium hydride (Alfa Aesar) was washed in pentane to remove the oil prior to usage.

Physical Measurements. UV-vis-NIR spectra were recorded on toluene or pyridine solutions using a Perkin–Elmer Lambda 800 Spectrometer. Electrospray ionization mass spectrometry (ESI-MS) and gas chromatography mass spectrometry (GC/MS) were performed at the Mass Spectrometry Facility at University of California, Irvine. X-band EPR spectra ($B_1 \perp B_0$) were collected using Bruker EMX spectrometer equipped with ER041XG microwave bridge. ⁵⁷Fe Mössbauer spectra were measured on liquid nitrogen cooled samples at zero magnetic field with a constant acceleration spectrometer (SEE Co., Edina, MN).

[ONO^q]FeCl₂ (1)

A suspension of FeCl₃ (1.131 g, 6.973 mmol, 1 equiv.) in 75 mL toluene at 77 K was treated with K[ONO^q] (3.217 g, 6.975 mmol, 1 equiv.). The reaction was allowed to warm to ambient temperature (24 °C) with constant stirring. After stirring for 15 hours at ambient temperature, the solids were removed by vacuum filtration and washed with toluene. The combined toluene fractions were then concentrated to 50 mL and recrystallized by adding pentane and cooling to –30 °C overnight. Dark brown solids were obtained in 71% yield (2.70 g). Anal. Calc. for

$C_{28}H_{40}NO_2Cl_2Fe$: C, 61.22; H, 7.34; N, 2.55; Found: C, 60.99; H, 7.25; N, 2.48. MS (ESI⁻) m/z : 548.14 (M^+). UV-vis-NIR (toluene) λ_{max}/nm ($\epsilon/ M^{-1} cm^{-1}$): 318 (13,200), 456 (7,000), 840 (7,000), 930 (10,600).

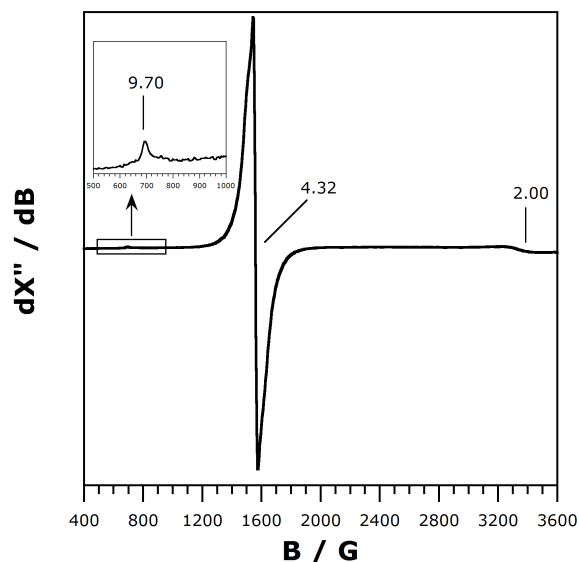


Figure S1. X-band EPR spectrum ($B_1 \perp B_0$) of $[ONO^q]FeCl_2$ (**1**) in toluene at 77 K.

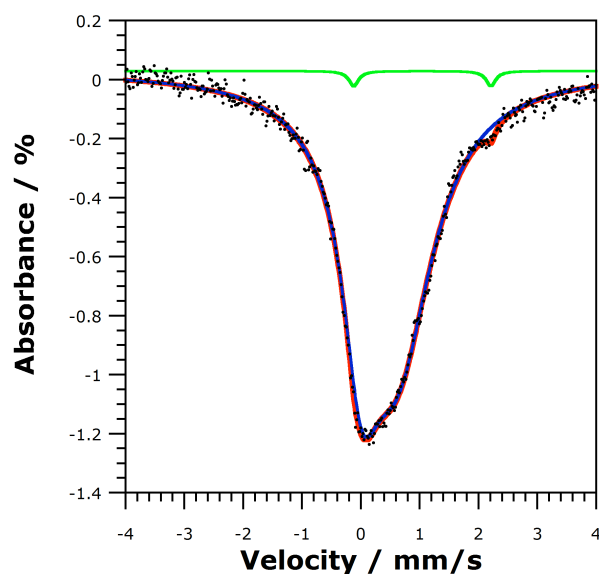


Figure S2. Mössbauer spectrum of $[ONO^q]FeCl_2$ (**1**) collected at 80 K. The spectral data corresponding to complex **1** (94%; IS = 0.3 mm/s; QS = 0.61 mm/s) is shown in blue while that of a small iron(II) impurity (6%; IS = 1.04 mm/s; QS = 2.33 mm/s) is shown in green. The overall fit of the data is shown in red.

[ONO^q]Fe[N(SiMe₃)₂]₂ (2)

A 50 mL pentane solution of FeCl(THF)[N(SiMe₃)₂]₂ (2.625 g, 5.691 mmol, 1 equiv.) and K[ONO^q] (2.744 g, 5.692 mmol, 1 equiv.) was stirred for 15 hours at ambient temperature. The solids were removed by vacuum filtration and washed with pentane. The combined pentane fractions were taken to dryness and the dark brown residue was recrystallized from a mixture of toluene and acetonitrile solution at -30 °C overnight. Dark brown solids were obtained in 65% yield (2.97 g). Anal. Calc. for C₄₀H₇₆N₃O₂Si₄Fe: C, 60.11; H, 9.58; N, 5.26; Found: C, 60.10; H, 9.82; N, 5.09. MS (ESI) *m/z*: 798.35 (M⁺). UV-vis-NIR (toluene) λ_{max}/nm (ε/ M⁻¹cm⁻¹): 458 (10,100), 872 (10,600), 914 (11,000).

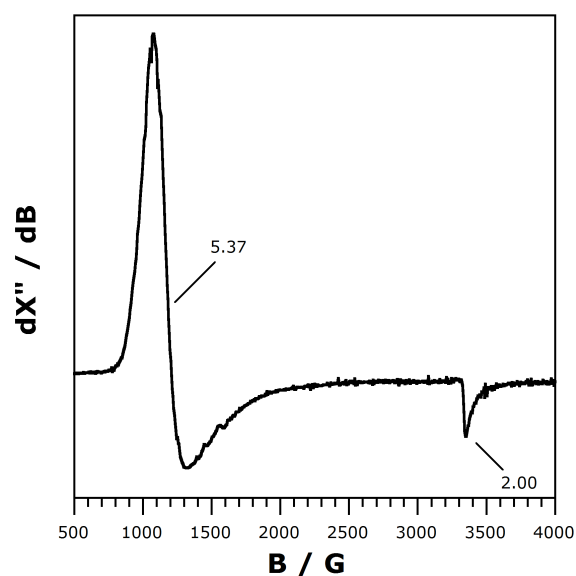


Figure S3. X-band EPR spectrum ($B_1 \perp B_0$) of [ONO^q]Fe[N(SiMe₃)₂]₂ (2) in toluene at 77 K.

[ONO^q]Fe(*ortho*-C₆O₂Cl₄)(py) (3) and {[ONO^q]Fe(*ortho*-C₆O₂Cl₄)}₂ (4)

A benzene solution of **2** (211 mg, 0.264 mmol, 1 equiv.) and tetrachlorocatechol (66 mg, 0.26 mmol, 1 equiv.) was stirred overnight (>12 hours) and the solvent was removed under reduced pressure to yield dark green residue. The residue was dissolved in diethylether pyridine (69.5 μL, 0.861 mmol, 3.26 equiv.) was added. The mixture stirred at room temperature for 30 minutes, after which it was cooled to -30 °C overnight to afford dark green solids of **3** in 63% yield (134 mg). UV-vis-NIR (toluene) λ_{max}/nm (ε/ M⁻¹cm⁻¹): 310 (5,100), 458 (5,100), 556 (3,000), 828 (4,500). Dissolving the dark green residue afforded after benzene removal in pentane and subsequent cooling of the solution to -30 °C afforded crystals of **4** suitable for X-ray diffraction in low yields.

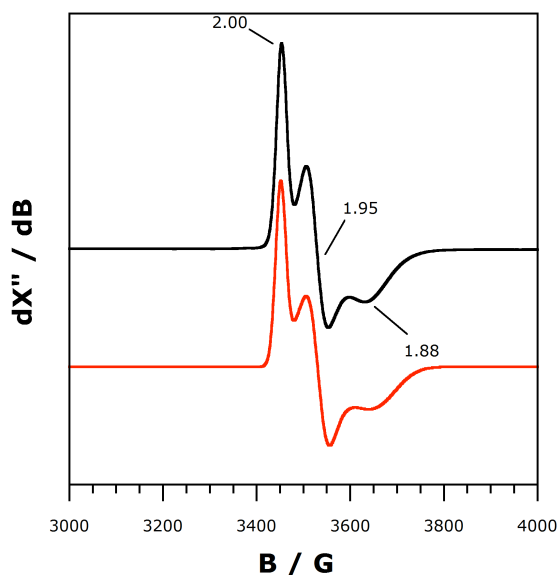


Figure S4. X-band EPR spectrum of [ONO^q]Fe(*ortho*-C₆O₂Cl₄)(py) (**3**) (black) in toluene at 4 K. The simulated spectrum is shown in red.

[ONO^{cat}]Fe(py)₃ (5) and {[ONO^{cat}]Fe(py)}₂ (6)

A freshly prepared sample of KC₈ (249 mg, 1.85 mmol, 2 equiv.) was suspended in 20 mL of THF, pyridine (7.5 mL, 93 mmol, 101 equiv.) was added and the solution was frozen in a liquid nitrogen cold well. The solution was thawed and solid **1** (507 mg, 0.924 mmol, 1 equiv.) was added immediately. The reaction mixture was allowed to warm to ambient temperature with stirring, which continued for 18 hours. Solid graphite was removed by filtration and washed with toluene. The combined green toluene fractions were combined and taken to dryness to afford a dark green solid. This residue was recrystallized from liquid-liquid diffusion of

acetonitrile into a pyridine solution of the complex at $-30\text{ }^{\circ}\text{C}$. Complex **5** was isolated as dark green microcrystalline solids in 74% yield (490 mg). UV-vis-NIR (pyridine) $\lambda_{\text{max}}/\text{nm}$ ($\epsilon/\text{M}^{-1}\text{cm}^{-1}$): 342 (sh; 12,200), 384 (6,700), 432 (sh; 4,100), 504 (sh; 2,700), 618 (2,300), 1137 (3,000). Recrystallization of **5** from toluene in the absence of excess pyridine at $-30\text{ }^{\circ}\text{C}$ afforded diiron complex **6**.

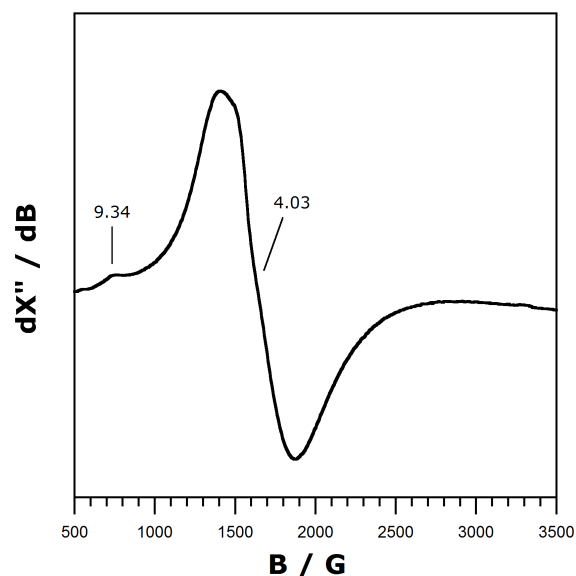


Figure S5. X-band EPR spectrum of $[\text{ONO}^{\text{cat}}]\text{Fe}(\text{py})_3$ (**5**) in pyridine at 77 K.

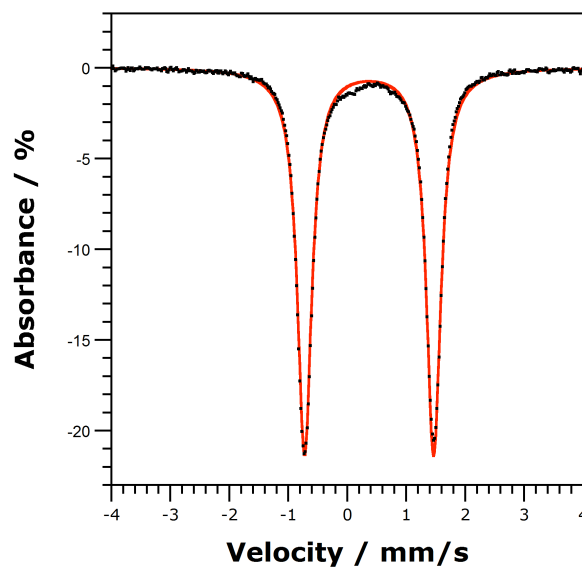


Figure S6. Mössbauer spectrum of $[\text{ONO}^{\text{cat}}]\text{Fe}(\text{py})_3$ (**5**) collected at 90 K (IS = 0.37 mm/s; QS = 2.19 mm/s).

Analytical Quantification Procedures

The reactions of **2** with ^tBuSH and N₂H₂Ph₂ reactions were monitored via gas chromatography mass spectrometry (GC/MS) to quantify the formation of ^tBuS–S^tBu and PhN=NPh, respectively. Calibration curves were generated for benzene solutions azobenzene (0.000500–0.00250 mM) and di-*tert*-butyl disulfide (0.000414–0.00207 mM), containing 1,2-bis(4-methylphenyl)diazene (0.00150 mM) and diisopropyl disulfide (0.0314 mM), respectively, as internal standards to correct for changes to injection volume.

Quantification of di-*tert*-butyl disulfide in the reaction of **2** with ^tBuSH.

To a thawing solution of **2** (0.251–0.253 mmol, 1 equiv.) in 15 mL benzene and pyridine (2.0 mL, 25 mmol, 100 equiv), *tert*-butylthiol (57 μL, 0.51 mmol, 2 equiv.) was added. The dark brown-green solution was stirred at ambient temperature for 16 hours, after which a 1 mL aliquot of the reaction mixture was taken to prepare a 100 mL benzene solution. From this stock solution, three 10 mL benzene solutions of the GC-MS samples were prepared, each containing 1 mL aliquot of the stock solution and known amounts of the internal standard.

These steps were repeated two more times, generating a total of nine samples that were then injected into the GC-MS instrument. The average yield of the di-*tert*-butyl disulfide was determined to be 81% based on initial quantities of **2**.

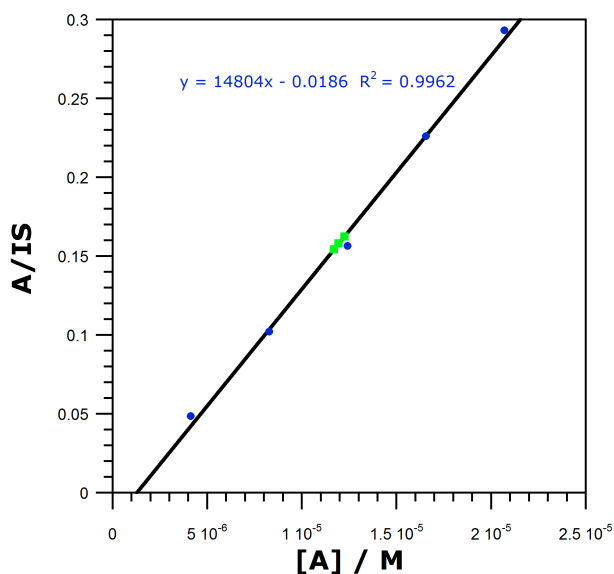


Figure S7. Plot of calibration curve (blue) and quantification of di-*tert*-butyl disulfide (green). A/IS describes the ratio of analyte peak area (A): internal standard peak area (IS). [A] corresponds to the concentration of di-*tert*-butyl disulfide.

Quantification of azobenzene

To a thawing solution of **2** (0.251 mmol, 1 equiv.) in 15 mL benzene and pyridine (2.0 mL, 25 mmol, 100 equiv), diphenylhydrazine (12 mg, 0.25 mmol, 1 equiv.) was added. The dark brown-green solution was stirred at ambient temperature for 16 hours, after which a 1 mL aliquot of the reaction mixture was taken to prepare a 100 mL benzene solution. From this solution, three 10 mL benzene solutions of the GC-MS samples were prepared, each containing 1 mL aliquot of the stock solution and known amounts of the 1,2-bis(4-methylphenyl)diazene internal standard. These steps were repeated two more times, generating a total of nine samples that were then injected into the GC-MS instrument. The average yield of the azobenzene was determined to be 94% based on initial quantities of **2**.

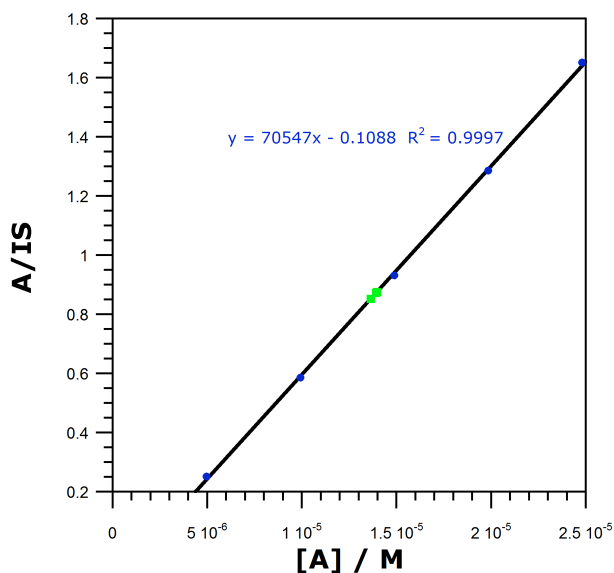


Figure S8. Plot of calibration curve (blue) and quantification of azobenzene (green). A/IS describes the ratio of analyte peak area (A): internal standard peak area (IS). [A] corresponds to the concentration of azobenzene.

Crystallographic Methods

X-ray diffraction data were collected on crystals mounted on glass fibers using a Bruker CCD platform diffractometer equipped with a CCD detector. Measurements were carried out using Mo K α ($\lambda = 0.71073 \text{ \AA}$) radiation, which was wavelength selected with a single-crystal graphite monochromator. A full sphere of data was collected for each crystal structure. The APEX2 program package was used to determine unit-cell parameters and to collect data.⁶ The raw frame data were processed using SAINT⁷ and SADABS⁸ to yield the reflection data files. Subsequent calculations were carried out using the SHELXTL⁹ program suite. Structures were solved by direct methods and refined on F² by full-matrix least-squares techniques to convergence. Analytical scattering factors for neutral atoms were used throughout the analyses. Hydrogen atoms, though visible in the difference Fourier map, were generated at calculated positions and their positions refined using the riding model. ORTEP diagrams were generated using ORTEP-3 for Windows¹⁰ and all thermal ellipsoids are drawn at the 50% probability level. Diffraction collection and refinement data for **1-6** are shown in Table S1 and complete crystallographic data are available from the Cambridge Crystallographic Data Center (CCDC 916892-916897).

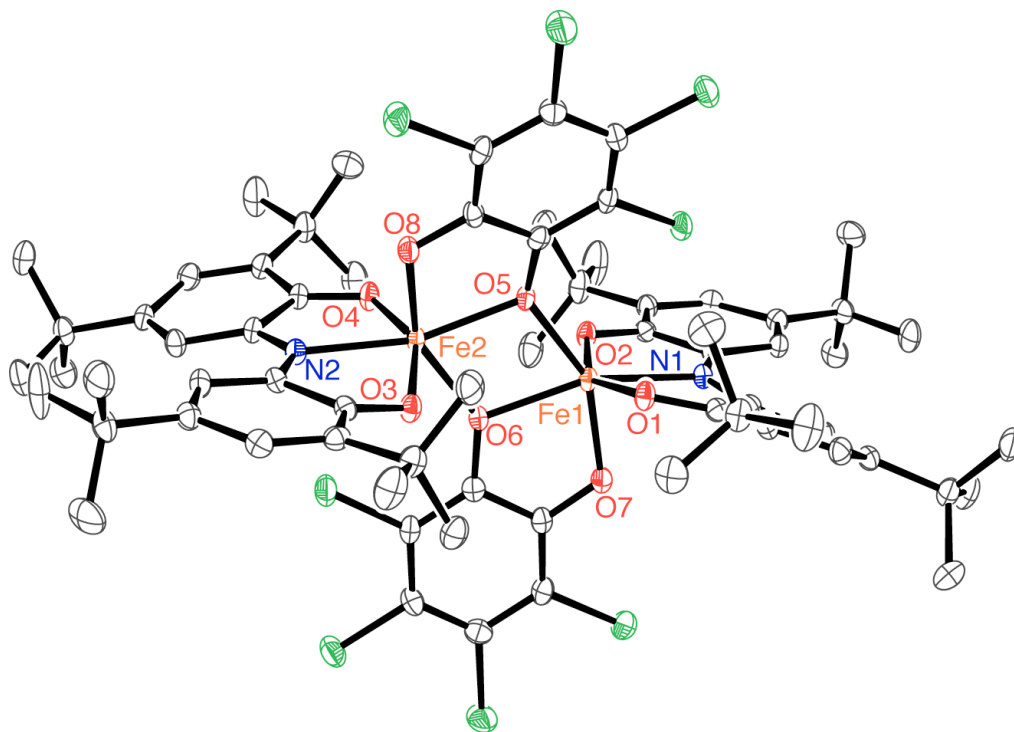


Figure S9. ORTEP diagram of $\{[\text{ONO}^q]\text{Fe}(\text{ortho-C}_4\text{O}_2\text{Cl}_4)\}_2$ (**4**). Ellipsoids are displayed at 50% probability. Hydrogen atoms and solvent molecules are omitted for clarity.

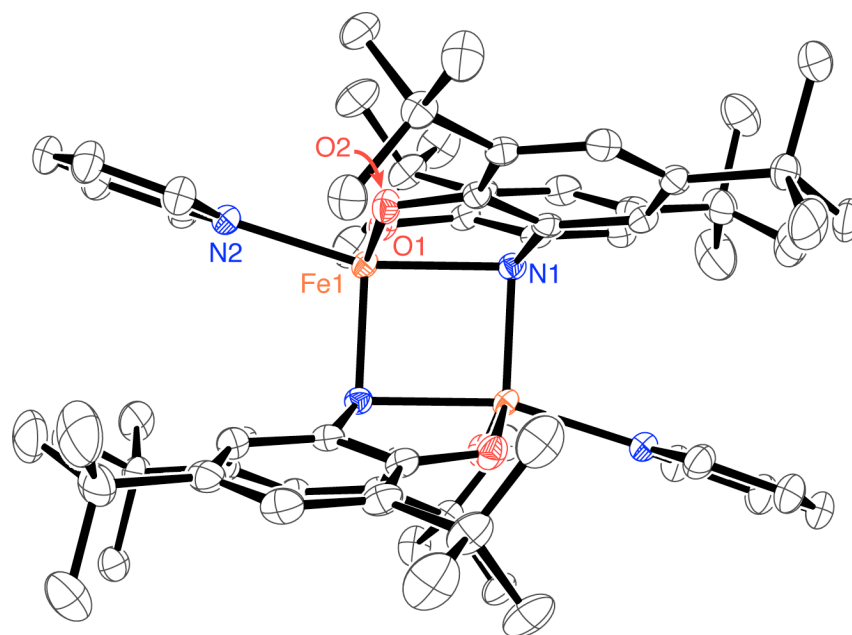


Figure S10. ORTEP diagram of $\{[\text{ONO}^{\text{cat}}]\text{Fe}(\text{py})\}_2$ (**6**). Ellipsoids are displayed at 50% probability. Hydrogen atoms and solvent molecules are omitted for clarity.

Table S1. X-Ray Diffraction Data Collection and Refinement Parameters for [ONO⁰]FeCl₂ (1), [ONO⁰]Fe[N(SiMe₃)₂] (2), [ONO⁰]Fe(ortho-C₄O₂Cl₄)(py) (3), {[ONO⁰]Fe(ortho-C₄O₂Cl₄)₂} (4), [ONO⁰]Fe(py)₃ (5), {[ONO⁰]Fe(py)₂} (6), [ONO⁰]FeCl₂·C₇H₈ (1·C₇H₈) [ONO⁰]Fe[N(SiMe₃)₂] (2) [ONO⁰]Fe(py)₃·C₂H₃N (5·C₂H₃N) {[ONO⁰]Fe(py)₂} (6)

	[ONO ⁰]FeCl ₂ ·C ₇ H ₈ (1·C ₇ H ₈)	[ONO ⁰]Fe[N(SiMe ₃) ₂] (2)	[ONO ⁰]Fe(ortho-C ₄ O ₂ Cl ₄) ₂ (3·C ₇ H ₈)	[ONO ⁰]Fe(ortho-C ₄ O ₂ Cl ₄)(py) ₃ (4·1.5 C ₅ H ₇)	{[ONO ⁰]Fe(ortho-C ₄ O ₂ Cl ₄) ₂ } (4·1.5 C ₅ H ₇)	[ONO ⁰]Fe(py) ₃ ·C ₂ H ₃ N (5·C ₂ H ₃ N)	{[ONO ⁰]Fe(py) ₂ } (6)
Empirical formula	C ₃₃ H ₄₉ NO ₂ Cl ₂ Fe	C ₄₀ H ₇₆ N ₃ O ₂ Si ₄ Fe	C ₄₃ H ₅₅ Cl ₄ FeN ₃ O ₅	C ₁₅₁ H ₁₀₆ C ₁₁₈ Fe ₄ N ₄ O ₁₆	C ₄₃ H ₅₈ N ₃ O ₂ Fe	C ₆₆ H ₉₀ Fe ₂ N ₄ O ₄	
Formula weight	641.49	799.25	877.54	1556.86	756.81	1115.12	
Crystal system	Monoclinic	Monoclinic	Monoclinic	Triclinic	Monoclinic	Monoclinic	
Space group	<i>P</i> 2 ₁ / <i>n</i>	<i>P</i> 2 ₁ / <i>c</i>	<i>P</i> 2 ₁ / <i>n</i>	<i>P</i> $\bar{1}$	<i>P</i> 2 ₁	<i>P</i> 2 ₁ / <i>c</i>	
<i>T</i>	143(2) K	143(2) K	88(2) K	143(2) K	88(2) K	143(2) K	
<i>a</i>	10.1903(6) Å	11.9269(7) Å	12.6068(11) Å	14.8709(8) Å	14.0101(6) Å	14.1943(10) Å	
<i>b</i>	12.5783(8) Å	17.5744(10) Å	24.431(2) Å	15.7470(8) Å	15.7187(7) Å	14.2798(10) Å	
<i>c</i>	27.2498(17) Å	24.1583(13) Å	16.6177(14) Å	17.9214(10) Å	19.9340(8) Å	17.1104(13) Å	
α	90°	90°	90°	94.0663(7)°	90°	90°	
β	96.2952(8)°	111.5826(6)°	111.8027(9)°	111.4278(7)°	97.6912(5)°	113.9953(9)°	
γ	90°	90°	90°	95.5142(7)°	90°	90°	
<i>V</i>	3470.4(4) Å ³	4708.75 Å ³	4752.1(7) Å ³	3863.0(4) Å ³	4350.38 Å ³	3168.4(4) Å ³	
<i>Z</i>	4	4	4	2	4	2	
Reflections collected	36819	11228	46245	42365	47597	33737	
data/restraints/parameters	7105 / 0 / 468	11228 / 0 / 756	8703 / 11 / 498	15780 / 0 / 893	17560 / 1 / 981	6485 / 0 / 355	
R1 [<i>I</i> > 2σ(<i>I</i>)] ^a	0.0341	0.0297	0.0610	0.0401	0.0354	0.0413	
wR2 (all data) ^a	0.0802	0.0737	0.1709	0.0999	0.0877	0.1125	
GOF ^b	1.026	1.032	1.019	1.074	1.008	1.014	

^a R1 = Σ|F_o - |F_c||Σ|F_o|; wR2 = [Σ[w(F_o² - F_c²)²]/Σ[w(F_o²)]^{1/2}; GOF = [Σw(|F_o - |F_c||²)/(n - m)]^{1/2}

References

- 1) I. S. Weitz and M. Rabinovitz *J. Chem. Soc. Perkin Trans.* **1993**, *1*, 117–120.
- 2) R. A. Zarkesh, J. W. Ziller, A. F. Heyduk *Angew. Chem. Int. Ed.* **2008**, *47*, 4715–4718.
- 3) G. Szigethy, D. W. Shaffer, A. F. Heyduk *Inorg. Chem.* **2012**, [Online early access]. DOI: 10.1021/ic2026076. Published Online: Apr 6, 2012.
- 4) S. Laha and R. G. Luthy *Environ. Sci. Technol.* **1990**, *24*, 363–373.
- 5) T. Deschner, K. W. Törnroos, R. Anwänder *Inorg. Chem.* **2011**, *50*, 7217–7228.
- 6) APEX2, Version 2008.3-0 / 2.2-0, Bruker AXS, Inc.; Madison, WI 2007.
- 7) SAINT Version 7.53a / 7.46a, Bruker AXS, Inc.; Madison, WI 2007.
- 8) Sheldrick, G. M. *SADABS*, Version 2007/4, Bruker AXS, Inc.; Madison, WI 2007.
- 9) Sheldrick, G. M. *SHELXTL*, Version 6.12; Bruker AXS, Inc.: Madison, WI, 2001.
- 10) International Tables for X-Ray Crystallography 1992, Vol. C., Dordrecht: Kluwer Academic Publishers.